ANALELE UNIVERSITĂȚII
"EFTIMIE MURGU" REȘIȚA
ANUL XIX, NR. 1, 2012, ISSN 1453 - 7397

Carla Protocsil, Ionică Negru, Zeno-Iosif Praisach, Gilbert-Rainer Gillich

Considerations Regarding the use of Beam Models for Accurate Calculus of Natural Frequencies

The paper reflects the research performed by the authors, in destined to find out the proper beam model, in concordance with its geometrical characteristics. This knowledge is needed to establish the adequate relations in the difficult process of damage detection. First, we calculated the natural frequencies for two cases: the Euler-Bernoulli model and the Share model. Afterwards, using FEM simulations we determined these frequencies again. Comparison between analytic results and FEM analysis allow seeing which theoretical models best fit for the various investigated cases.

Keywords: *beam, natural frequency, FEM analysis, Euler-Bernoulli model, Share model*

1. Introduction

Application of non-destructive evaluation in the civil engineering involves the use on sensor networks to diagnose the health of large scale structures [1]. The concepts of defect and failure are general and have a very large mean. For a complete analysis of a structure, it is necessary to correctly identify damages and their causes, to find out the causal dependencies and to delimitate the particular causes from the common one.

Localization is important to simplify the repair and maintenance efforts. The conditions which determine the appearance of damages can be exaggerated external loads, humidity, temperature, vibration etc. Classification of damages can be made from the operability point of view: physical defects and functional defects. In the moment when appear a physical defect, all ensemble is break and no operational, while a functional defect appear in the moment when the system is operational, but it do not fulfill completely its function. Most of these defects are due to errors in the design and can be permanent or transient.

Our pervious researches made in the field of damage detection show that it is possible to detect damages in structures [2] and [3]; we also found a relation that correlates the natural frequencies with damage depth and position [4]. The method is generally available, but is applied differentiated for very long beams (modeled using the Euler-Bernoulli model) and beams of small length or high rigidity, where other models are involved.

In this paper is shows a comparison between the analytic results and experimental results for beams with various cross-sections and two levels of length:

- cross-sections of the beams - 11x11 mm; 13x13 mm; 14x14 mm; 16x16 mm; 20x20 mm;
- length 1000 mm and 2000 mm.

2. The analytical determination of frequencies

Trying to determine the exact natural frequencies of beams, a summary of the four beam theories is taken in consideration. The basic assumptions made by all these modes [5], are:

- one dimension (axial direction) is considerably larger than the other two;
- the material is linear elastic;
- the Poisson effect is neglected;
- the cross-sectional area is symmetric so that the neutral and centroidal axes coincide;
- planes perpendicular to the neutral axis remain perpendicular after deformation.
- the angle of rotation is small so that the small angle assumption can be used.

The four models consider more or less influences of external loads and strain [5], presented in table 1.

Table 1

Beam models	Bending moment	Lateral displacement	Shear deformation	Rotary inertia
Euler-Bernoulli	√	√	x	x
Rayleigh	√	√	x	√
Shear	√	√	√	x
Timoshenko	√	√	√	√

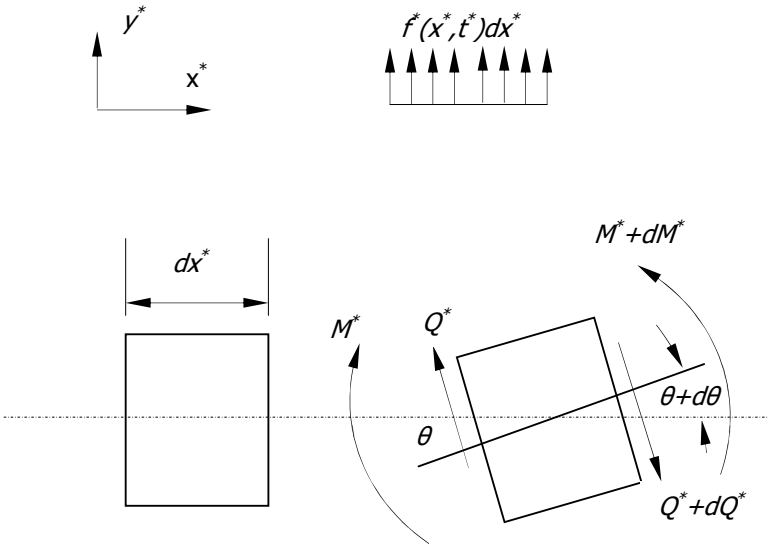

Figure 1. Incremental beam element

From the four theories of the dynamics of transversely vibration of beams we used two (Euler-Bernoulli and Shear) to analyze the beams with L_1 = 1000 mm and L_2 = 2000 mm respectively, having the cross-sections mentioned in the first chapter.

2.1. Natural frequency calculus using the Euler-Bernoulli model

To find the natural frequencies of the beams we started from the governing differential equation of motion, [3] and [5], given below:

$$\rho A \frac{\partial^2 v(x,t)}{\partial t^2} + \frac{\partial^4 v(x,t)}{\partial x^4} = f(x,t) \qquad (1)$$

where v is the vertical displacemet, ρ the mass density, A the cross-section area, x and t are variables in corespondence with dispakcement and time, and f stay for external loads.

The boundary condition to be satisfied by the cantilever beam, are:

- for clamped end : $\frac{\partial v}{\partial x} = 0$; $v = 0$

- for free end: $\frac{\partial^2 v}{\partial x^2} = 0$; $\frac{\partial^3 v}{\partial x^3} = 0$

Taking $f(x,t)=0$, and separating $v(x,t)$ into two functions such that $v(x,t)=W(x)T(t)$, the equation of motion (1) can be separated into two ordinary differential equations.

$$\left.\begin{aligned}\frac{d^2T(t)}{dt^2}+\omega^2T(t)=0\\ \frac{d^4W(x)}{dx^4}-\gamma^4W(x)=0\end{aligned}\right\} \quad (2)$$

γ is in correspondence with the angular frequency ω by:

$$\gamma^4=\rho A\omega^2 \quad (3)$$

From the second equations in (2) result the solution *W(x)* as following:

$$W(x)=C_1\sin\gamma x+C_2\cos\gamma x+C_3\sinh\gamma x+C_4\cosh\gamma x \quad (4)$$

where C_i are constant coefficients.

Deriving equation (4) three times, result a system of equastions for which, imposing the boundary conditions for a cantilever, results the relation to determin the natural frequencies as follows:

$$f_i=\frac{\lambda_i^2}{2\pi}\sqrt{\frac{EI}{\rho AL^4}} \quad (5)$$

where $\lambda_i=\gamma_i\cdot L$

Analyzing this beam the results shown in Table 2 and Table 3 were obtained.

Table 2

L_1 = 1000 mm					
Beam type / Mode *i*	**11x11**	**13x13**	**14x14**	**16x16**	**20x20**
1	8.9692	10.5999	11.4153	13.0460	16.3076
2	56.2089	66.4287	71.5386	81.7584	102.1980
3	157.3866	186.0023	200.3102	228.9260	286.1575
4	308.4151	364.4905	392.5282	448.6037	560.7546
5	509.8321	602.5288	648.8772	741.5740	926.9675
6	761.6010	900.0739	969.3103	1107.7832	1384.7290
7	1063.7236	1257.1279	1353.8300	1547.2343	1934.0429
8	1416.2001	1673.6910	1802.4365	2059.9274	2574.9093
9	1819.0305	2149.7632	2315.1296	2645.8625	3307.3281
10	2272.2144	2685.3443	2891.9092	3305.0391	4131.2989

Table 3

L_1 = 2000 mm					
Beam type / Mode *i*	11x11	13x13	14x14	16x16	20x20
1	2.2423	2.6500	2.8538	3.2615	4.0769
2	14.0522	16.6072	17.8847	20.4396	25.5495
3	39.3467	46.5006	50.0776	57.2315	71.5394
4	77.1038	91.1226	98.1321	112.1509	140.1887
5	127.4580	150.6322	162.2193	185.3935	231.7419
6	190.4003	225.0185	242.3276	276.9458	346.1823
7	265.9309	314.2820	338.4575	386.8086	483.5107
8	354.0500	418.4228	450.6091	514.9819	643.7273
9	454.7576	537.4408	578.7824	661.4656	826.8320
10	568.0536	671.3361	722.9773	826.2598	1032.824

2.2. Natural frequency calculus using the Shear model

This model adds the effect of shear distortion (but not rotary inertia) to the Euler-Bernoulli model. [5] The new variables are α – the angle of rotation of the cross-section due to the bending moment, β – the angle of distorsion due to shear. The total angle of rotation is approximately the first derivate of the deflection.

$$\alpha(x,t)+\beta(x,t)=\frac{\partial v(x,t)}{\partial x} \tag{6}$$

The equations of motion (using Hamilton's principle) are given by:

$$\left.\begin{aligned}\rho A\frac{\partial^2 v(x,t)}{\partial t^2}-k'GA\left(\frac{\partial^2 v(x,t)}{\partial x^2}-\frac{\partial \alpha(x,t)}{\partial x^2}\right)=f(x,t)\\ \frac{\partial^2 \alpha(x,t)}{\partial x^2}+k'GA\left(\frac{\partial v(x,t)}{\partial x}-\alpha(x,t)\right)=0\end{aligned}\right\} \tag{7}$$

where k' is a shape factor, and with the boundary conditions given by:

$$\left.\begin{aligned}\frac{\partial \alpha}{\partial x}\delta\alpha\Big|_0^1=0\\ k'GA\left(\frac{\partial v}{\partial x}-\alpha\right)\delta v\Big|_0^1=0\end{aligned}\right\} \tag{8}$$

in which: v is the displacement, α the angle of rotation due bending, $\frac{\partial \alpha}{\partial x}$ the moment, $k'GA\left(\frac{\partial v}{\partial x}-\alpha(x,t)\right)$ the shear.

The boundary conditions are:

- for the clamped end : $\alpha = 0; \nu = 0$
- for the free end : $\frac{\partial \alpha}{\partial x} = 0; k'GA\left(\frac{\partial \nu}{\partial x} - \alpha\right) = 0$

The two equations of motion (7) can be decupled to yield:

$$\frac{\partial^4 \nu(x,t)}{\partial x^4} - \frac{\rho}{k'G}\frac{\partial^4 \nu(x,t)}{\partial x^2 \partial t^2} + \rho A \frac{\partial^2 \nu(x,t)}{\partial t^2} = 0 \tag{9}$$

$$\frac{\partial^4 \alpha(x,t)}{\partial x^4} - \frac{\rho}{k'G}\frac{\partial^4 \alpha(x,t)}{\partial x^2 \partial t^2} + \rho A \frac{\partial^2 \alpha(x,t)}{\partial t^2} = 0 \tag{10}$$

Therefor, when $\nu(x,t)$ and $\alpha\ (x,t)$ are synchronized in time, results:

$$\begin{bmatrix} \nu(x,t) \\ \alpha(x,t) \end{bmatrix} = T(t)\begin{bmatrix} W(x) \\ \Psi(x) \end{bmatrix} \tag{11}$$

When $\begin{bmatrix} W(x) \\ \Psi(x) \end{bmatrix} = due^{rx}$, where

d – is the constant coefficient
u – is a vector of constant numbers
r – is the wave number,

we have that [5]:

$$\begin{bmatrix} k'GAr^2 + \rho A\omega^2 & -k'GAr \\ k'GAr & r^2 - k'GA \end{bmatrix} u = 0 \tag{12}$$

so, the mode shape r and eigenvectors u are obtained.

The determinant of the above matrix has to be zero, so:

$$r^4 + \frac{\rho\omega^2}{k'G}r^2 - \rho A\omega^2 = 0 \tag{13}$$

The wave numbers are given by:

$$r_i = \pm\sqrt{-\frac{\rho\omega^2}{2k'G} \pm \sqrt{\left(\frac{\rho\omega^2}{2k'G}\right)^2 + \rho A\omega^2}} \tag{14}$$

for i = 1,2,3,4...

Thus we have [5]:

$$u_i = \begin{bmatrix} k'GAr_i \\ k'GAr_i^2 + \rho A\omega^2 \end{bmatrix} \tag{15}$$

for i = 1,2,3,4...

From

$$\begin{bmatrix} W(x) \\ \Psi(x) \end{bmatrix} = \sum_{i=1}^{4} d_i u_i e^{r_i x} = d_1 u_1 e^{bx} + d_2 u_2 e^{-bx} + d_3 u_3 e^{iax} + d_4 u_4 e^{-iax} \tag{16}$$

we have

$$a = \sqrt{\frac{\rho\omega^2}{2k'G} + \sqrt{\left(\frac{\rho\omega^2}{2k'G}\right)^2 + \rho A\omega^2}}, \quad b = \sqrt{-\frac{\rho\omega^2}{2k'G} + \sqrt{\left(\frac{\rho\omega^2}{2k'G}\right)^2 + \rho A\omega^2}} \tag{17}$$

The natural frequency is given by [5]:

$$f = \frac{\sqrt{a^2 - b^2}}{2\pi} \sqrt{\frac{E}{\rho L^2}} \sqrt{\frac{k'}{2(1+\nu)}} \tag{18}$$

for i = 1,2,3,4...

The obtained results are presented in Table 4 and Table 5. Figure 2 present the differences between the natural frequencies determined by FE analysis and that obtained by analytical calculus.

Table 4

L_2 = 1000 mm					
Beam type / Mode *i*	**11x11**	**13x13**	**14x14**	**16x16**	**20x20**
1	8.968545	10.5989	11.4140	13.0441	16.3037
2	56.18085	66.3824	71.4808	81.6721	102.0295
3	157.1993	185.6934	199.9245	228.3506	285.0361
4	307.7373	363.3733	391.1339	446.5257	556.7118
5	508.0472	599.5887	645.2093	736.1129	916.3669
6	757.7169	893.6820	961.3406	1095.9313	1361.7871
7	1056.289	1244.9067	1338.6014	1524.6188	1890.4078
8	1403.222	1652.3841	1775.9053	2020.5888	2499.2880
9	1797.895	2115.1144	2272.0199	2582.0550	3185.1729
10	2239.613	2631.9853	2825.5794	3207.0536	3944.5528

Table 5

L_2 = 2000 mm					
Beam type / Mode *i*	**11x11**	**13x13**	**14x14**	**16x16**	**20x20**
1	2.2423	2.6499	2.8537	3.2614	4.0767
2	14.0505	16.6043	17.8810	20.4342	25.5390
3	39.3349	46.4813	50.0534	57.1954	71.4690
4	77.0613	91.0526	98.0446	112.0204	139.9339
5	127.3460	150.4475	161.9886	185.0493	231.0707
6	190.1561	224.6158	241.8248	276.1961	344.7212
7	265.4626	313.5097	337.4936	385.3716	480.7128
8	353.2304	417.0718	448.9231	512.4694	638.8402
9	453.4192	535.2354	576.0306	657.3669	818.8682
10	565.9827	667.9251	718.7223	819.9254	1020.532

We observe that on the first mode shape, the frequencies are similar, but on the superior mode shape begin to appear the differences. On shear we observe that the frequencies are smaller.

3. FEM analysis

We made the FEM analysis for length beam L_1 = 1000 mm and for length beam L_2 = 2000 mm, each with cross-section 20x20 and with meshes 2 and 5, the values are presented in Table 6.

Table 6

L_1 = 1000 mm				L_2 = 2 000 mm			
Beam type	**Mode *I***	**Mesh**		**Beam type**	**Mode *i***	**Mesh**	
		2	5			2	5
11x11	1	8.9732	8.9739	11x11	1	2.2429	2.2429
	2	56.2022	56.2070		2	14.0537	14.0543
	3	157.2254	157.2393		3	39.3419	39.3436
	4	307.6937	307.7217		4	77.0689	77.0723
	5	507.7750	507.8228		5	127.3459	127.3515
	6	756.9489	757.0230		6	190.1326	190.1412
	7	1054.6291	1054.7369		7	265.3913	265.4036
	8	1400.1276	1400.2770		8	353.0768	353.0935
	9	1792.6637	1792.8639		9	453.1366	453.1587
	10	2231.3720	2231.6332		10	565.5116	565.5399

Table 6 (continued)

13x13	1	10.6052	10.6062	13x13	1	2.6507	2.6509
	2	66.4092	66.4159		2	16.6086	16.6094
	3	185.7130	185.7322		3	46.4898	46.4921
	4	363.2561	363.2951		4	91.0594	91.0640
	5	599.0679	599.1350		5	150.4377	150.4455
	6	892.3172	892.4217		6	224.5629	224.5749
	7	1242.0541	1242.2065		7	313.3729	313.3900
	8	1647.1736	1647.3858		8	416.7933	416.8168
	9	2106.4337	2106.7189		9	534.7385	534.7696
	10	2618.4713	2618.8443		10	667.1119	667.1521
14x14	1	11.4213	11.4224	14x14	1	2.8547	2.8548
	2	71.5104	71.5178		2	17.8859	17.8868
	3	199.9383	199.9598		3	50.0627	50.0653
	4	390.9671	391.0110		4	98.0504	98.0556
	5	644.5276	644.6033		5	161.9721	161.9809
	6	959.5961	959.7144		6	241.7524	241.7659
	7	1334.9988	1335.1719		7	337.3140	337.3334
	8	1769.3767	1769.6183		8	448.5643	448.5909
	9	2261.2100	2261.5352		9	575.3970	448.5909
	10	2808.8399	2809.2658		10	717.6922	717.7379
16x16	1	13.0534	13.0544	16x16	1	3.2626	3.2627
	2	81.7066	81.7132		2	20.4403	20.4411
	3	228.3442	228.3632		3	57.2059	57.2082
	4	446.2259	446.2644		4	112.0225	112.0271
	5	735.0192	735.0849		5	185.0139	185.0216
	6	1093.2360	1093.3374		6	276.0721	276.0838
	7	1519.1653	1519.3115		7	385.0822	385.0989
	8	2010.8459	2011.0468		8	511.9072	511.9300
	9	2566.1086	2566.3748		9	656.3902	656.4202
	10	3182.6145	3182.9573		10	818.3551	818.3934
20x20	1	16.3177	16.3193	20x20	1	4.0785	4.0787
	2	102.0711	102.0814		2	25.5476	25.5488
	3	284.9526	284.9825		3	71.4804	71.4840
	4	555.9972	556.0577		4	139.9205	139.9276
	5	914.0544	914.1580		5	230.9729	230.9850
	6	1356.3613	1356.5212		6	344.4382	344.4567
	7	1879.7603	1879.9907		7	480.0944	480.1209
	8	2480.7140	2481.0298		8	637.6797	637.7159
	9	3155.4053	3155.8220		9	816.8962	816.9438
	10	3899.8297	3900.3634		10	1017.4118	1017.4728

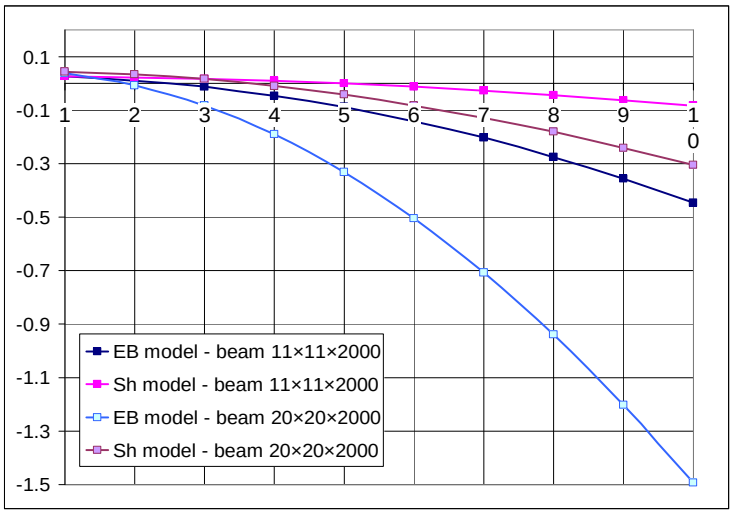

Figure 2. Relative deviation between the first ten natural frequencies obtained by FEM analysis and calculated using the Euler-Bernoulli and Share model respectively – beam of length 2000 mm

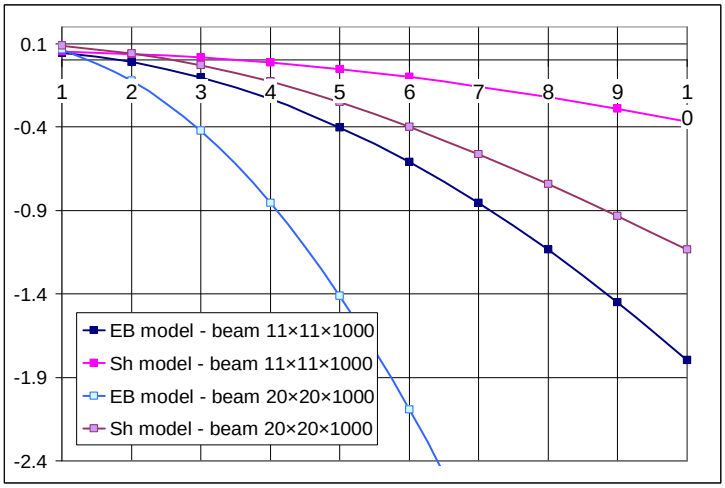

Figure 3. Relative deviation between the first ten natural frequencies obtained by FEM analysis and calculated using the Euler-Bernoulli and Share model respectively – beam of length 1000 mm

We observe, in figure 2, that for the beam of length 2000 mm the Share model is proper for both presented cases (11×11 and 20×20), presenting deviations less than 0.3% for all 10 weak-axis bending vibration modes. For the beam with length 2000 mm and cross-section 11×11 the Euler-Bernoulli model is proper too, while for more rigid beams (i.e. 20×20) it provides deviations up to 1.5% in higher vibration modes.

The results for the shorter beam with length 1000 mm, presented in figure 3, reveal that for applications needing accurate results the Share model can be involved for beams with reduced rigidity (i.e. 11×11), deviations being less than 0.4%. For more rigid beams deviations are significant even for this model, therefore the use of Timoshenko model is recommended. The Euler-Bernoulli model cannot be used for short beams at all.

4. Conclusion

The researches presented in this paper confirm that as shorter and rigid the beam, the Euler-Bernoulli model dose not provide enough precise information regarding the natural frequencies and mode shapes and the Share model is necessary to be involved. Moreover, for more severe cases, like the beam of length 1000 mm and cross-section 20×20 mm, a improved model, like the Timoshenko one is needed.

Acknowledgement

The work has been funded by the Sectoral Operational Programme Human Resources Development 2007-2013 of the Romanian Ministry of Labour, Family and Social Protection through the Financial Agreement POSDRU/88/1.5/S/61178 and POSDRU/107/1.5/S/76813.

References

[1] Berinde C.F., Gillich G.R., Chioncel C.P., *Structure monitoring and evaluation using vibro-acoustic method supported by the Wigner-Ville Distribution*, Romanian Journal of Acoustics and Vibration 7, 2006.

[2] Gillich G.R., Birdeanu D., Gillich N., Amariei D., Iancu V., Jurcau C.S. *Detection of damages in simple elements*, Proceedings of the 20th International DAAAM Symposium 20 (1), Vienna, 2009.

[3] Gillich G.R., Praisach Z.I., Moaca-Onchis D., - *About the effectiveness of damage detection methods based on vibration measurements,*

3rd WSEAS International Conference on Engineering Mechanics, Structures, Engineering Geology, Corfu Island, 2010.
[4] Praisach Z., Gillich G.-R., Birdeanu D. *Considerations on Natural Frequency Changes in Damaged Cantilever Beams Using FEM*, 3rd WSEAS International Conference on Engineering Mechanics, Structures, Engineering Geology, Corfu Island, 2010.
[5] Seon M. Han, Haym Bernaroya, Timothy Wei *Dynamics of Transversely Vibrating Beams Using Four Engineering Theories,* Journal of Sound and Vibration, 1999.
[6] Mănescu, T. Şt. , Nedelcu, D. – *Analiză structurală prin metoda elementului finit*, Editura Orizonturi universitare, Timişoara, 2005.
[7] Gillich G.R. *Dinamica masinilor. Modelarea sistemelor tehnice*, Editura AGIR, Bucuresti, 2003.

Addresses:

- Eng. Carla Protocsil, "Eftimie Murgu" University of Reşiţa, Piaţa Traian Vuia, nr. 1-4, 320085, Reşiţa, c.protocsil@uem.ro
- Eng. Ionică Negru, "Eftimie Murgu" University of Reşiţa, Piaţa Traian Vuia, nr. 1-4, 320085, Reşiţa, negru_ionica@yahoo.com
- Dr.Eng. Zeno-Iosif Praisach, "Eftimie Murgu" University of Reşiţa, Piaţa Traian Vuia, nr. 1-4, 320085, Reşiţa, z.praisach@uem.ro
- Prof.Dr.Eng. Gilbert-Rainer "Eftimie Murgu" University of Reşiţa, Piaţa Traian Vuia, nr. 1-4, 320085, Reşiţa, gr.gillich@uem.ro